

Time-Variant Structural Performance of the Certosa Cable-Stayed Bridge

Fabio Biondini, Assoc. Prof., Politecnico di Milano, Milan, Italy; **Dan M. Frangopol**, Prof. and F. R. Khan Endowed Chair of Structural Engineering and Architecture, Lehigh University, Bethlehem, Pennsylvania, USA – formerly, Prof., University of Colorado, Boulder, Colorado, USA; **Pier Giorgio Malerba**, Prof., Politecnico di Milano, Milan, Italy

Summary

This paper presents the time-variant structural performance evaluation of the Certosa cable-stayed bridge built in Milan, Italy. Since the pylons showed some traces of damage, a rehabilitation intervention has been carried out after fifteen years of lifetime. In order to investigate the effectiveness of the rehabilitation intervention, a novel procedure for the durability analysis of concrete structures subjected to diffusive attacks from external aggressive agents is applied. Based on this procedure, both the deterministic and probabilistic time-variant structural performances are analyzed with respect to proper indicators considering two separate cases: without and with rehabilitation intervention. The direct comparison of the results demonstrates that the adopted intervention enhances the structural performance over time and reduces its dispersion effects.

Introduction

In recent years, a growing number of concrete cable-stayed bridges exhibits extensive damage due to the interaction with the environment. In fact, the damaging process induced by the diffusive attack of environmental aggressive agents usually leads to deterioration of concrete and corrosion of reinforcement [1]. In cable-stayed bridges, damage tends to develop in both the deck and the pylons. However, the effects of the deterioration of the pylons are usually more important since the percentage of damaged material volume contained in such elements is greater than in the deck. Clearly, this aspect is emphasized in bridges with very slender pylons.

This study is concerned with the Certosa cable-stayed bridge built in Milan, Italy (Fig. 1). Since its pylons showed some traces of damage, a rehabilitation intervention has been carried out after fifteen years of lifetime. In order to investigate the effectiveness of the rehabilitation, the time-variant performance of the pylons is evaluated in both deterministic and

probabilistic terms. The numerical simulation exploits the potentialities of a novel procedure recently proposed by the authors for the durability analysis and lifetime assessment of concrete structures in aggressive environments [2, 3]. In particular, the time evolution of the structural performance of the damaged pylons, already investigated in previous studies [4, 5], is compared with the performance resulting after the rehabilitation intervention. The results of such a comparison provide a basis for informed decision-making

concerning the next inspection and maintenance actions, together with a collection of information for a future comparative evaluation of the structural integrity of the Certosa cable-stayed bridge.

The Certosa Cable-Stayed Bridge

Design Requirements and Strategies

The cable-stayed bridge over the Milan-Certosa railway-junction was erected at the end of 1980s [6]. The Certosa bridge represents a particular application of this kind of structure, oriented to the solution of the problems of urban viability. The main design requirements were: (a) deck cross-section with maximum depth of 1,60 m; (b) maximum reduction of any interference with the rail traffic during all the building stages (foundations, piers, deck); (c) preliminary evaluation of the costs, required by the Italian State Railways, caused by the slowing down of the trains. In addition, Milan's

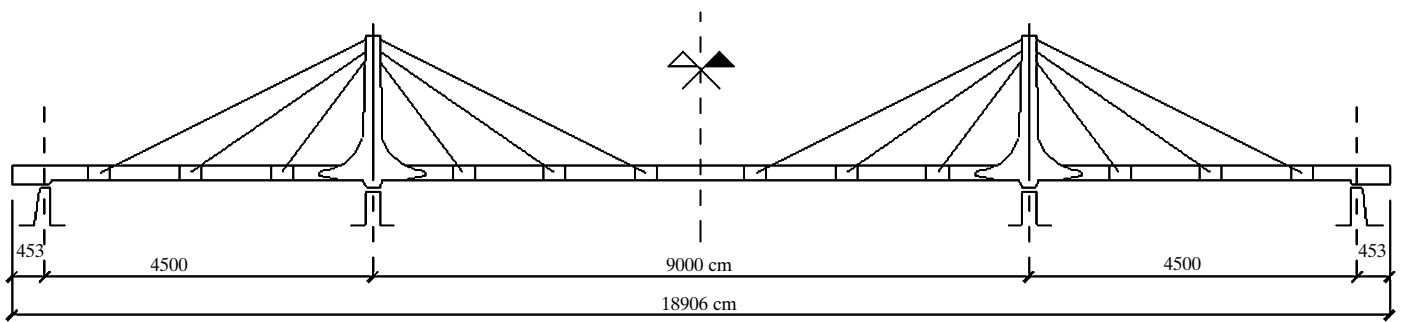


Peer-reviewed by international experts and accepted for publication by SEI Editorial Board

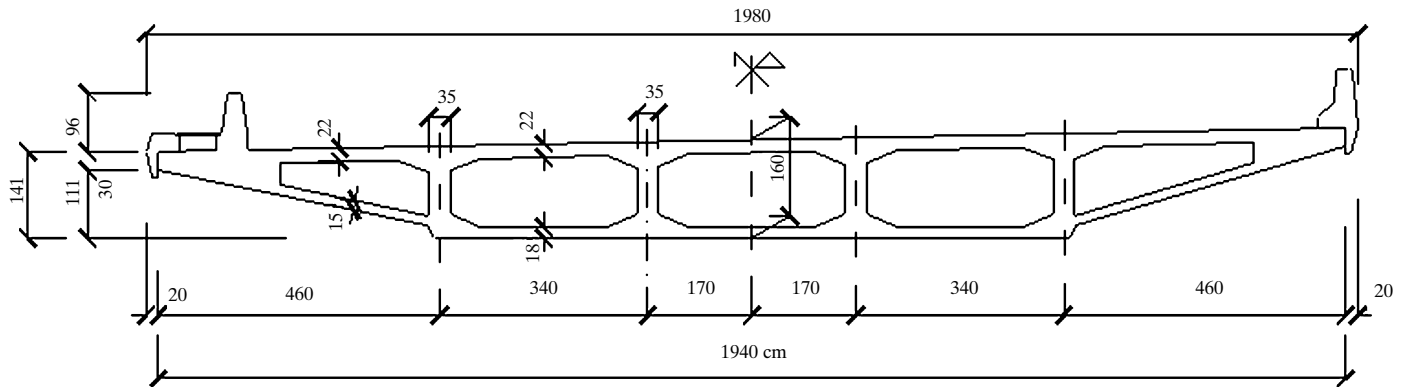
Paper received: August 22, 2005
Paper accepted: February 6, 2006



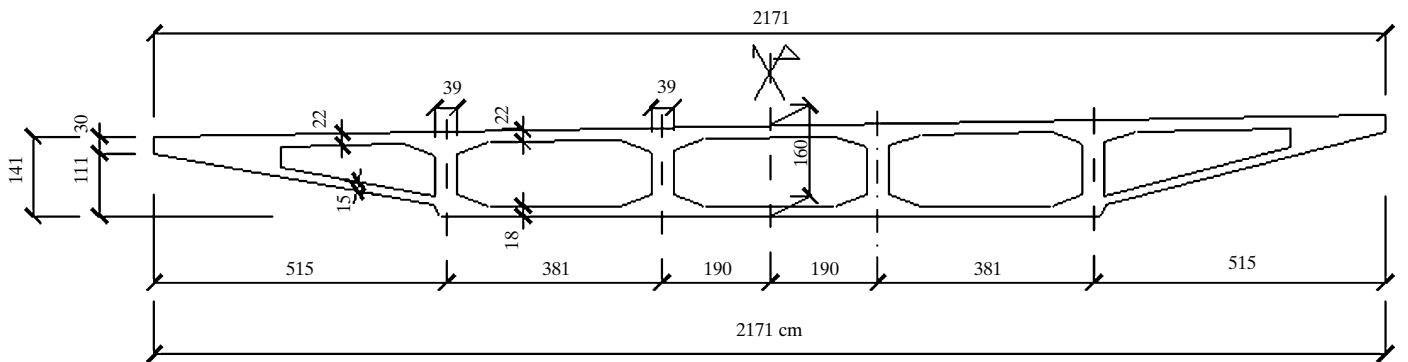
Fig. 1: View of the Certosa cable-stayed bridge



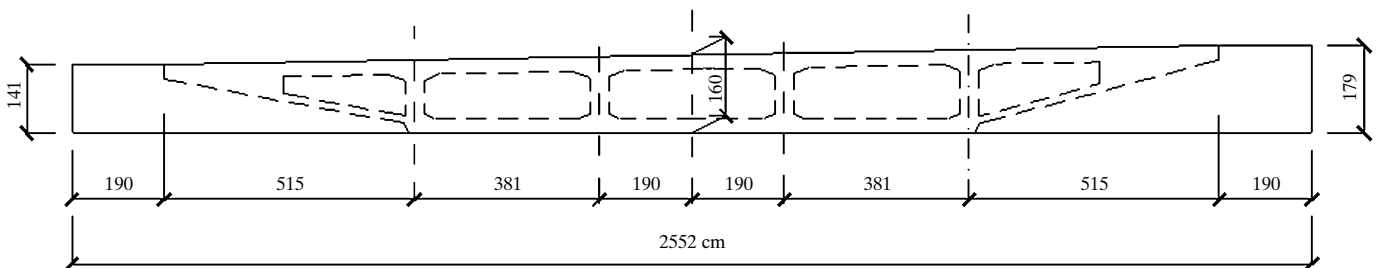
(a) Main dimensions of the bridge



(b) Straight cross-section of the deck



(c) Skewed cross-section of the deck



(d) Skewed cross-section on the transversal beam with the heads of the cable anchorages at the ends

Fig. 2: Certosa cable-stayed bridge

Municipality required that the erection of the new bridge had to be executed next to an existing old arch concrete bridge (three 25 m span arches) which must, in the meantime, continue its service.

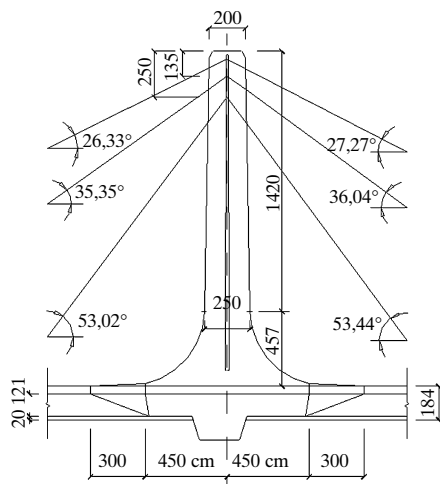
Several design alternatives were examined. Among them, a solution based on a cable-stayed bridge with three spans of 45-90-45 m (Fig. 2a) and with a deck 1,60 m deep (Fig. 2b, c, d) was finally selected. The suspension system is fan-shaped and consists of 8 stays for each pylon. The height of the two pylons

with respect to the deck level is about 19 m (Fig. 3a). The use of the cable-stayed bridges over spans less than about 200 m may appear a bit forced. In this case, however, this kind of solution reduced most of the interference with the rail traffic and allowed an autonomous organization of the construction for almost the whole structure. In fact, the erection procedure was unusual, in that it involved firstly the construction of the structure in two halves outside the rail area and then their assembly. When the structure was in place, the two halves

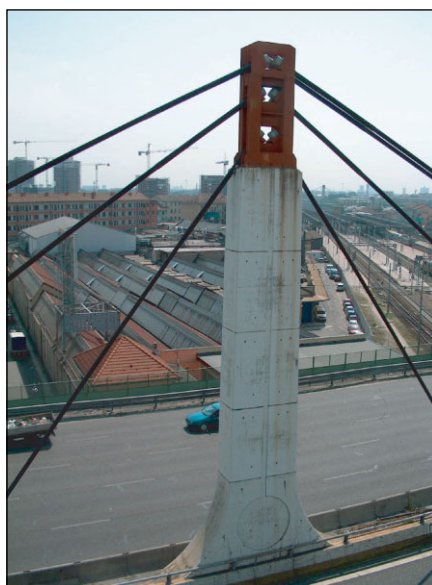
were made continuous by means of a connection casting and prestressing cables.

Bridge Characteristics

The total length of the bridge is 180 m, with a central span of 90 m and two lateral spans of 45 m, as shown in Fig. 2a. The bridge deck is a five cells box girder, 19,80 m wide and 26,7° skewed with respect to the road axis. The transversal section has a depth varying from 1,40 m to 1,80 m and the upper slab has the same small transversal



(a) Main geometrical dimensions



(b) View of a pylon after 15 years of lifetime

Fig. 3: The bridge pylons

slope as the road (Fig. 2b,c). The upper and lower slabs are 0,22 m and 0,18 m thick, respectively. Along its span the box is stiffened by a set of transversal beams (Fig. 2d), placed in correspondence to the stays. Such beams finish with two short cantilevers to which the stays are anchored. The transversal beams over the piers are deeper than the others, to hold the high forces transmitted by the pylons. The deck and the beams are prestressed with cables made up of 14 and 19 strands of 0,6 inches.

The pylons of the cable-stayed bridge are 19,00 m high and have a rectangular cross-section, varying along the height from $1,14 \times 2,00$ m at the top to $1,14 \times 2,50$ m at the bottom (Fig. 3a). The tapered shape of the frontal view finishes in two corbels, which were planned to lift the bridge. The ends of the pylons carry the devices used to anchor the stays. There are in total three seats consisting of steel boxes, which make it possible to anchor the stays leaving them, crossed but not intersected on the same plane.

Each pylon has three pairs of stays, skewed with respect to the horizontal plane as shown in Fig. 3a. The stays are composed, the longest to the shortest, by 2×45 , 60, 45 strands of 0,6 inches. The prestressing of the stays was defined to balance the time dependent effects associated to creep and shrinkage of the concrete deck [7]. The stress in the stays under dead loads is then expected to be nearly constant in time.

Structural Rehabilitation of the Pylons

After about fifteen years of service, the Milan Municipality decided for a general and detailed inspection of the bridge. The accurate design of the shape of the surfaces and the care spent in the reinforcement detailing, in the determination of an adequate cover thickness and in the choice of effective surface protective materials have contributed to the conservation of this bridge. Even though the structure had to withstand the severe loading conditions acting on the most important and busy access to Milan, it was in general in a good state. The deck was intact and presented surfaces without cracks, spallings or salt patches. Traces of damage were visible on the most exposed parts, including the four pylons, surrounded by the wind flow and subjected to the flow of acid rain and to the attack of aggressive materials coming from both the road and the underlying railway (Fig. 3b).

Inspection Activities

The first inspections revealed that some dramatic appearances of the surface crack patterns were due mainly to the traces of a mix of oil and dust retained by the lips of paint skin, delaminated from the concrete surface. The local removal of the paint revealed (a) small size reticulates of cracks, marked by dark contours but without a measurable width and (b) small width cracks randomly distributed (Fig. 4a). These effects can be attributed to the plas-

tic shrinkage and to the water loss during the first phases of the curing process. Cracks of same importance have been detected close to massive casts (Fig. 4b) and to the boundaries of the second phase completion casts. After a strong sandblasting cleaning (Fig. 5a), a set of carbonation and hardening tests have been carried out. During these activities it was not possible to take out boring samples. The depth of carbonation resulted in accordance with the expected values on a 15 year old structure (min. 6,7 mm, max. 20,5 mm, average value 10,3 mm). The rebound hammer tests provided medium/high values of the RH index (min. 43,89; max. 57, average value 50,17). At the basis of the cast interruption some aggregate segregation has been detected, but with the aggregates strongly adherent among themselves through the residual cement paste (Fig. 4c). Spalling and initial steel corrosion have been detected only at the lower external parts of the pylons, which are directly exposed to traffic emissions (Fig. 4d).

Repair Interventions

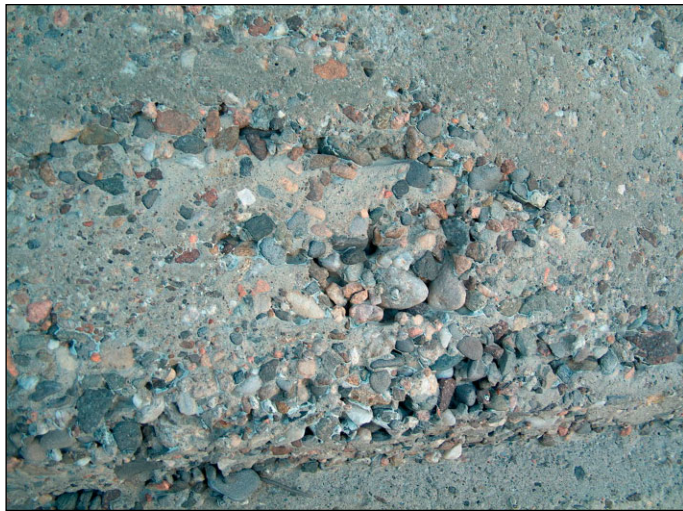
The guideline of the rehabilitation operations is summarized herein. The main cracks have been curved up to the basis of the crack (Fig. 5b) and then sutured with tixotropic, anti-shrinkage, polypropylene fiber reinforced high strength mortar (Cubic Compression Strength $R_{28} > 55,2$ N/mm². Flexural Strength $> 11,1$ N/mm²) (Fig. 5c). The small cracks and the segregation zones have been repaired with high adhesion cement mortar, added with small polyvinilalcohol fibers (Adhesion Strength $> 3,0$ N/mm²) (Fig. 5d). The whole skin surfaces have been protected with high adhesion, high elasticity cement mortar ($E_{28} = 9000$ N/mm²), reinforced with double or simple skin mesh (Fig. 5e). This protection contributes to contrast the restart of carbonation and it is transpiring outward and waterproof inward. The final surface was painted with a silicate non-pellicular paint that is also transpiring outward and waterproof inward (Fig. 5f). In this way, future diffusive attacks of external aggressive agents are prevented. Finally, also a detailed inspection of the head anchorages has been carried out (Fig. 6a). The steel anchorage assembly has been painted with a 65 μ m enamel composed by polyuretanic resins (Fig. 6b). Fig. 7 shows a global view of a pylon after the rehabilitation interventions.



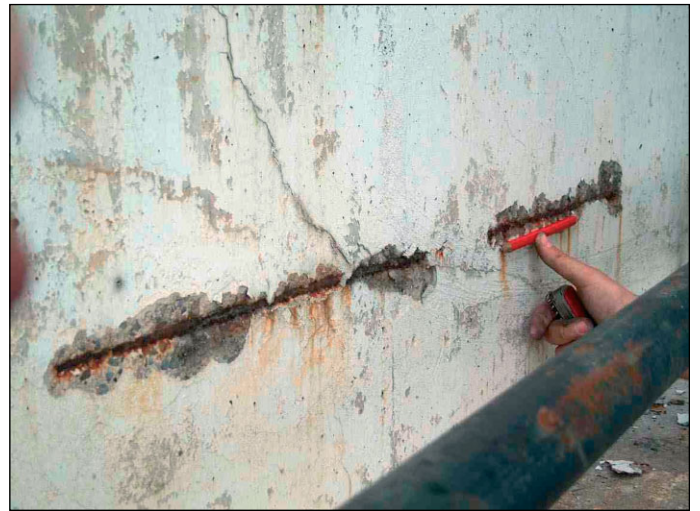
(a) Randomly distributed cracks



(b) Localized crack



(c) Aggregate segregation



(d) Spalling and initial steel corrosion

Fig. 4: Traces of structural damage of the pylons revealed by the inspection activities

Time Variant Structural Performance

The time-variant structural performance of the Certosa bridge is investigated by means of a novel methodology recently proposed by the authors for durability analysis of concrete structures subjected to the diffusive attack from external aggressive agents. This methodology is based on a proper formulation of deteriorating reinforced concrete finite beam elements, which include the coupling effects between the diffusion process and the cracking state. In this way, in contrast to the usual approaches dealing with the local deterioration of the materials only, the proposed methodology allows to account for the redistribution of the internal forces due to the time evolution of deterioration and, consequently, to evaluate the global effects of the local damaging phenomena on the overall performance of the structure [2].

However, it is worth noting that in the present case no considerable redistribution effects are expected, especially in the pylons. In fact, as already mentioned, prestressing of the stays was designed in such a way that the stress level under dead loads is maintained approximately constant. In addition, despite the effects of performance deterioration, the stress level under dead loads has been successfully checked during time with a periodical monitoring activity. For this reason, the time-variant structural performance of the bridge is evaluated by focusing the attention on the cross-section at the base of the pylons, where the most evident traces of deterioration were present. Such cross-section, shown in Fig. 8a, has main nominal dimensions $d_y = 2,50$ m and $d_z = 1,14$ m, and is reinforced with 86 bars having nominal diameter $\varnothing = 26$ mm.

In the following, the performance of the pylons is investigated up to 50 years of

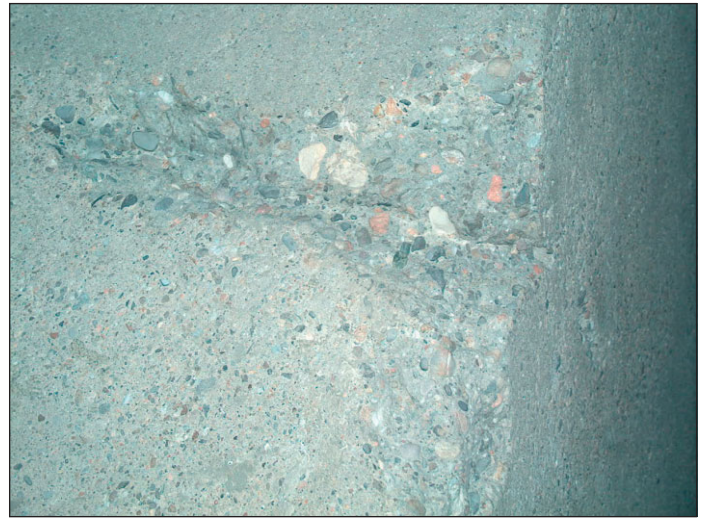
lifetime by considering two scenarios. In the first one, the structure is left free to undergo damage without any intervention. In the second one the effects of the rehabilitation are taken into account after fifteen years of service by (a) assuming an undamaged state for the restored layer of the concrete cover and (b) placing a diffusive barrier along the boundary of the cross-section in such a way that diffusion from outside is stopped and future damage can be induced only by the agent already existing inside the structure.

Simulation of the Diffusion Process

The kinetic diffusion process of the environmental agents is described according to the Fick's laws [8] and is effectively simulated by using cellular automata [9]. In particular, it can be shown that the Fick's laws in d -dimensions ($d = 1,2,3$) can be reproduced by



(a) Sandblasting



(b) Local curving up to the basis of the crack



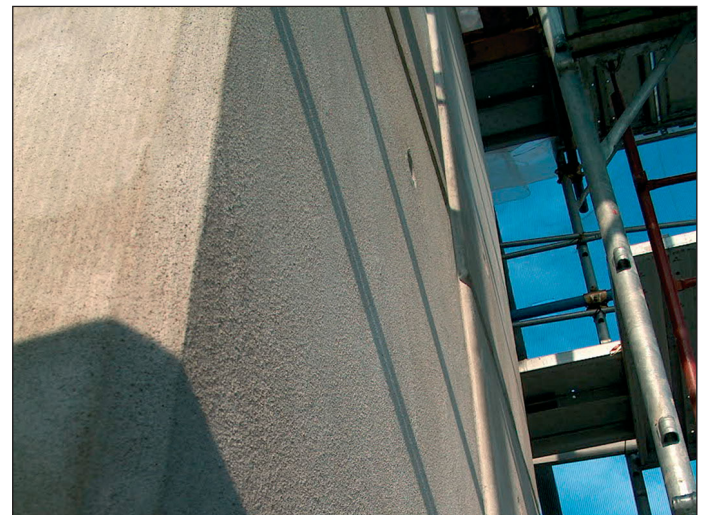
(c) Local sutures with tixotropic, anti-shrinkage, polypropylene fiber reinforced mortar



(d) Small local damage (segregation, small cracks) repairs with high adhesion cement mortar, added with polyvinilalcohol fibers



(e) Skin protection with high adhesion elasticity sealing cement mortar, reinforced with double or simple skin mesh



(f) Pylon surface after skin protection

Fig. 5: Repair of the whole surfaces of the pylons

adopting the following evolutionary rule [2]:

$$C_i^{k+1} = \phi_0 C_i^k + \frac{1-\phi_0}{2d} \sum_{j=1}^d (C_{i-1,j}^k + C_{i+1,j}^k) \quad (1)$$

where the discrete variable $C_i^k = C(\mathbf{x}_i, t_k)$ represents the concentration of the component in the cell i at time t_k , and ϕ_0 is a suitable evolutionary coefficient. The deterministic value

$\phi_0 = 1/2$ usually leads to a good accuracy of the automaton. However, ϕ_0 must be modeled as a random variable to take into account the stochastic effects in the diffusion process.



(a) Head of the anchorage cable inspection

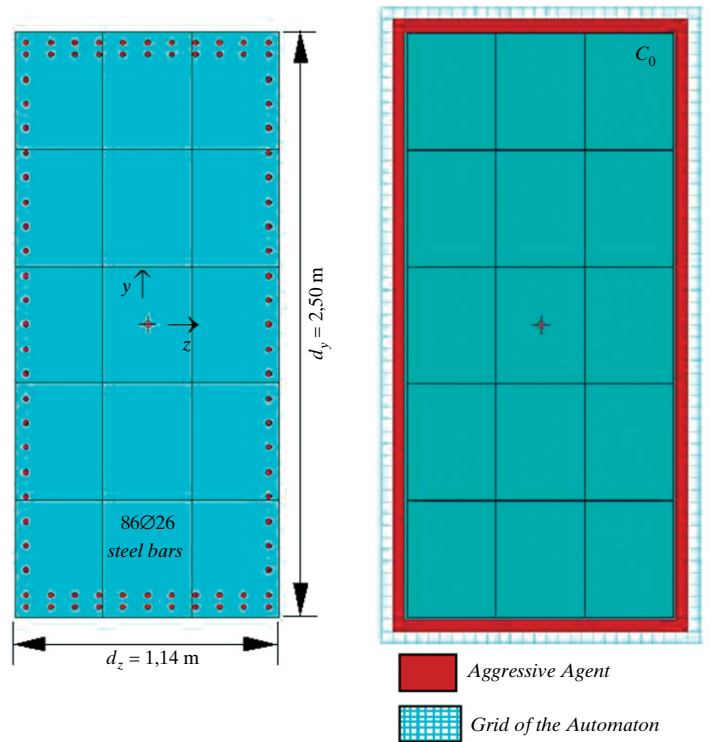
Fig. 6



(b) Detail of the anchorage assembly after painting



Fig. 7: View of a pylon after the rehabilitation intervention



(a) Model, dimensions and reinforcement

(b) Grid of the automaton and location of the aggressive agent

Fig. 8: Cross-section at the base of the pylons

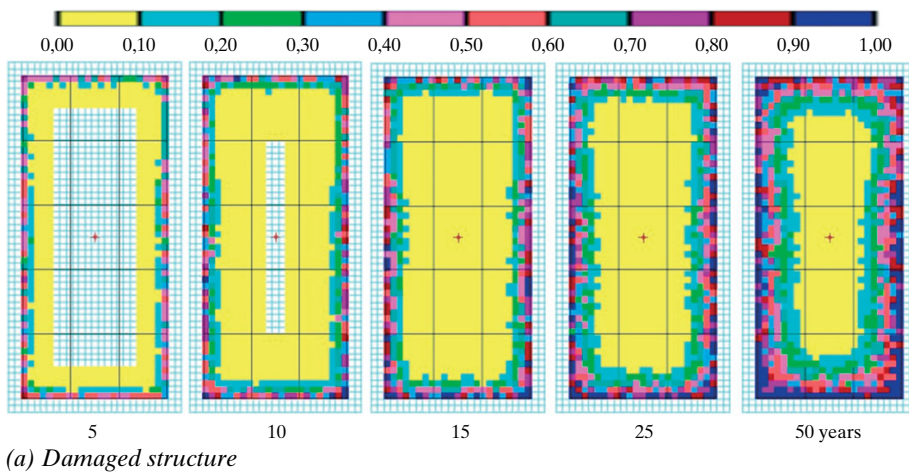
Moreover, to regulate the process according to a given diffusivity coefficient D , a proper discretization in space and time should be chosen in such a way that the grid dimension Δx and the time step Δt satisfy the following relationship [2]:

$$D = \frac{1 - \phi_0}{2d} \frac{\Delta x^2}{\Delta t} \quad (2)$$

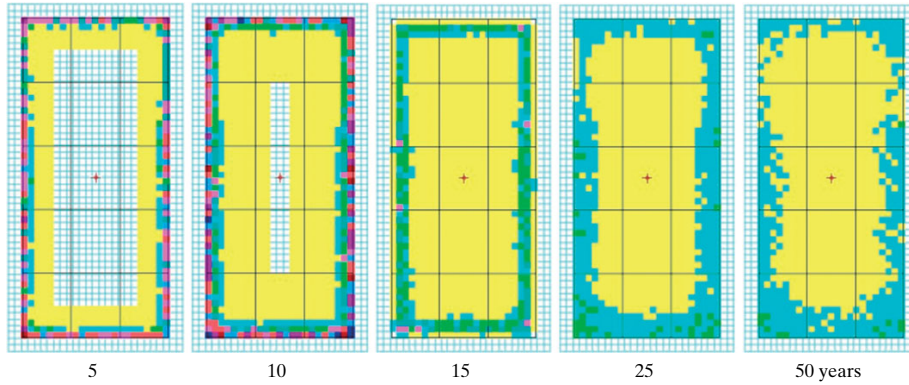
The cellular automaton associated to the considered cross-section is shown

in Fig. 8b. With reference to a nominal diffusivity coefficient $D = 10^{-11} \text{ m}^2/\text{sec}$, the automaton is defined by a grid dimension $\Delta x = 50,2 \text{ mm}$ and a time step $\Delta t = 1 \text{ year}$. The aggressive agent is assumed to be located along the whole external perimeter of the cross-section with concentration $C(t) = C_0$. For the purpose of the present study the thickness of the restored layer has been assumed equal the grid dimension (50,2 mm) in order to comply with the adopted modeling.

The diffusion process associated with the two investigated scenarios, without and with rehabilitation intervention, is described by the maps of concentration $C(\mathbf{x},t)/C_0$ of the aggressive agent shown in Fig. 9. The direct comparison of the concentration maps in Fig. 9a and 9b highlights the high effectiveness of the rehabilitation intervention with regards to the limitation of the diffusive attack of the aggressive agent.



(a) Damaged structure



(b) Rehabilitated structure

Fig. 9: Maps of concentration $C(\mathbf{x},t)/C_0$ of the aggressive agent after 5, 10, 15, 25, and 50 years from the initial time of diffusion penetration

Modeling of Structural Damage

Structural damage is modeled by introducing a degradation law of the effective resistant area for both the concrete matrix and the steel bars. This degradation is achieved by means of proper dimensionless *damage indices* δ_c and δ_s , respectively, which provide a direct measure of the damage level of the materials within the range [0; 1].

The damaging processes in concrete structures undergoing diffusion are, in general, very complex. Moreover, the available information about environmental agents and material characteristics is usually not sufficient for a detailed modeling. However, despite the complexity of the diffusion process and the lack of sufficient data, simple degradation models can often be successfully adopted. In this study, the

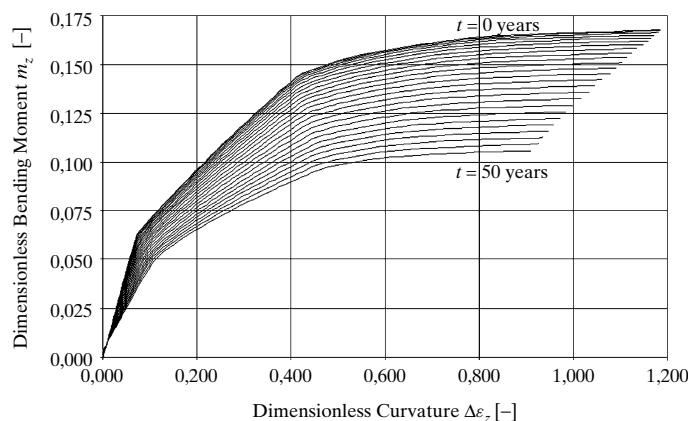
damage indices $\delta_c = \delta_c(\mathbf{x}, t)$ and $\delta_s = \delta_s(\mathbf{x}, t)$ at point $\mathbf{x} = (y, z)$ and time t are correlated to the diffusion process by assuming, for both materials, a linear relationship between the rate of damage and the mass concentration $C = C(\mathbf{x}, t)$ of the aggressive agent:

$$\frac{\partial \delta_c(\mathbf{x}, t)}{\partial t} = \frac{C(\mathbf{x}, t)}{C_c \Delta t_c} \quad (3)$$

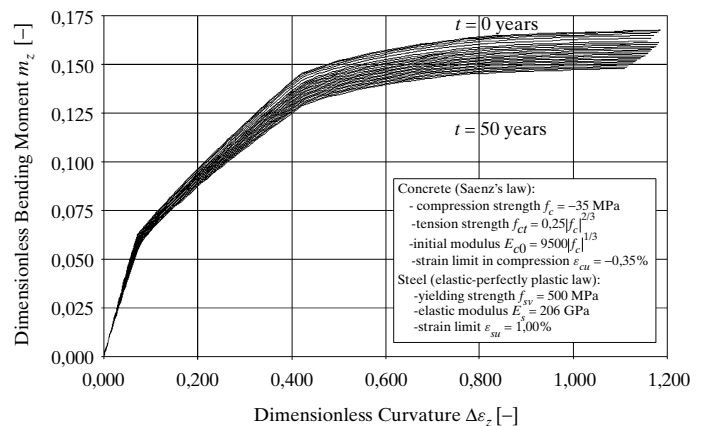
$$\frac{\partial \delta_s(\mathbf{x}, t)}{\partial t} = \frac{C(\mathbf{x}, t)}{C_s \Delta t_s}$$

where C_c and C_s represent the values of constant concentration $C(\mathbf{x}, t)$ which lead to a complete damage of the materials after the time periods Δt_c and Δt_s , respectively. In addition, the initial conditions $\delta_c(\mathbf{x}, t_0) = \delta_s(\mathbf{x}, t_0) = 0$ with $t_0 = \max\{t \mid C(\mathbf{x}, t) \leq C_{cr}\}$ are assumed, where C_{cr} is a critical threshold of concentration. Since the rate of mass diffusion depends on the stress state, the interaction between diffusion process and mechanical behavior of the damaged structure is also taken into account by a proper modeling of the random variable ϕ_0 , which describes the stochastic effects in the mass transfer [2]. The nominal values $C_{cr} = 0$, $C_c = C_s = C_0$, $\Delta t_c = 25$ years and $\Delta t_s = 50$ years, are adopted here.

The mechanical damage induced by diffusion can be evaluated from Fig. 10, which shows for the two investigated scenarios the time evolution of the dimensionless bending moment $m_z = M_z / (f_c A_{c0} d_y)$ versus curvature $\Delta \varepsilon_z = 100 \chi_z d_y$ diagrams under the axial force $n = N / (f_c A_{c0}) = -0,201$, where $N = -20$ MN. The nominal values of the main parameters which define the non-linear constitutive laws of the materials are also listed in Fig. 10b. The direct comparison of the diagrams in

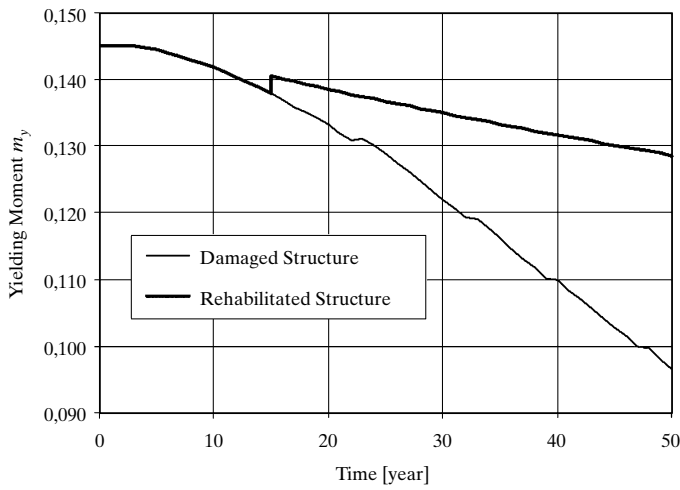


(a) Damaged structure

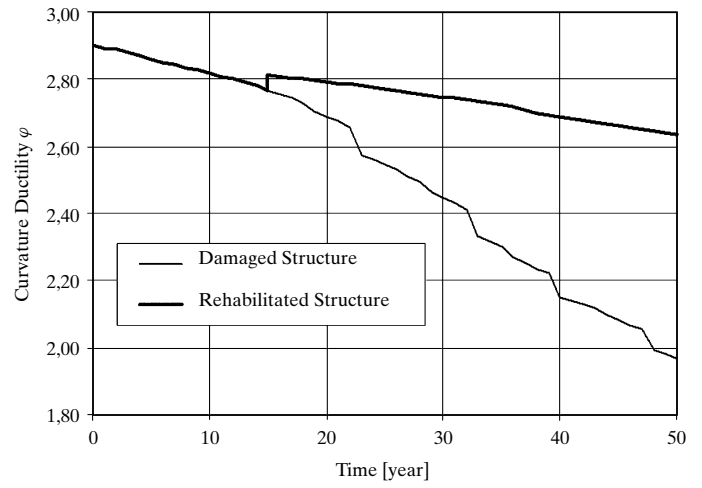


(b) Rehabilitated structure

Fig. 10: Time evolution of bending moment $m_z = M_z / (f_c A_{c0} d_y)$ / curvature $\Delta \varepsilon_z = 100 \chi_z d_y$ diagrams during the first 50 years of lifetime ($\Delta t = 2$ years)



(a) Yielding moment



(b) Curvature ductility

Fig. 11: The realization of a single sample of time evolution

Fig. 10a and 10b highlights the high effectiveness of the rehabilitation intervention with regards to the degradation of the structural performance induced by the aggressive agents.

With reference to these diagrams, several parameters could be adopted as suitable measures of the structural performance. Meaningful parameters are for example the values of the bending moment at yielding m_y , and the curvature ductility $\varphi = \chi_u/\chi_y$ given by the ratio of curvatures at ultimate and yielding. The time evolution of such performance indicators is given in the diagrams of Fig. 11. Such diagrams show that the adopted rehabilitation intervention leads not only to an increase of structural performance, but, mainly, to a relevant decrease of the rate of deterioration and, consequently, to a significant reduction of

the costs related to future inspections and maintenance activities.

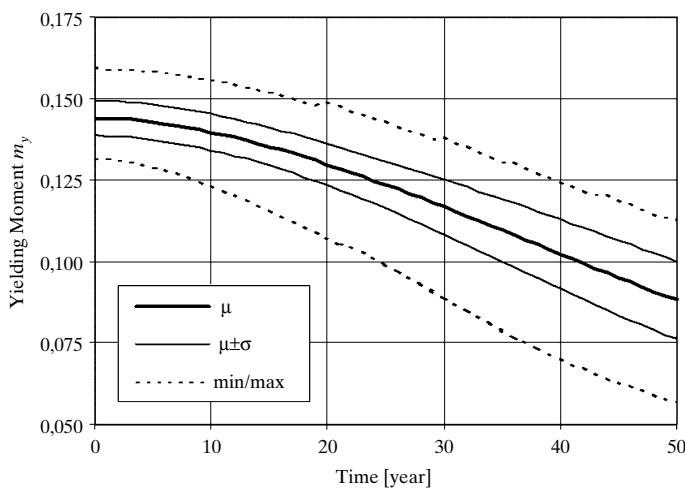
Such a comparison makes the beneficial effects of rehabilitation very clear from a qualitative point of view. However, the previous deterministic results cannot be used for reliable quantitative predictions because of the unavoidable sources of uncertainty involved in the problem. For this reason, in the following a probabilistic assessment of the service life is carried out and the comparison between the two scenarios is made by taking several uncertainties into account.

Probabilistic Analysis and Lifetime Assessment

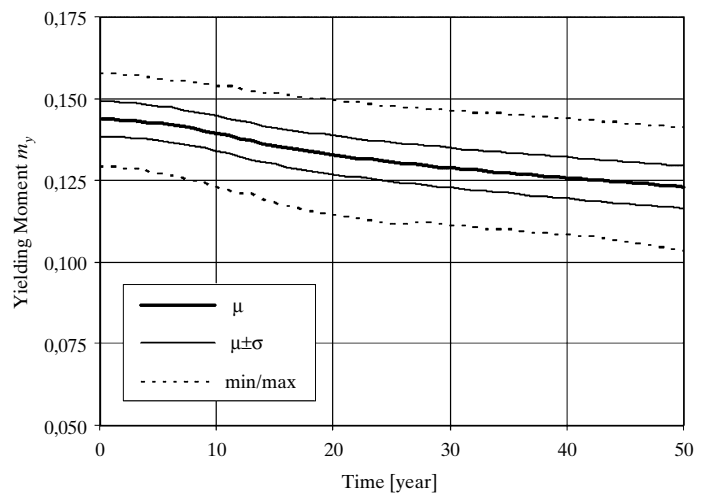
The probabilistic model for the service life assessment assumes as

random variables the material strengths f_c and f_{sy} , the coordinates (y_p, z_p) of the nodal points $p = 1, 2, \dots$ which define the two-dimensional model of the concrete cross-section, the coordinates (y_m, z_m) and the diameter \varnothing_m of the steel bars $m = 1, 2, \dots$, the diffusion coefficient D , and the damage rates $q_c = (C_c \Delta t_c)^{-1}$ and $q_s = (C_s \Delta t_s)^{-1}$. These variables are assumed to have the probabilistic distribution with the mean μ and standard deviation σ values listed in Table 1 [3].

A probabilistic measure of the time-variant structural performance is achieved by Monte Carlo simulation. The sampling process is based on the antithetic variables technique and the goodness of the sample size is evaluated by means of a posteriori error estimation. With reference to a sample of 2000 simulations for each one of

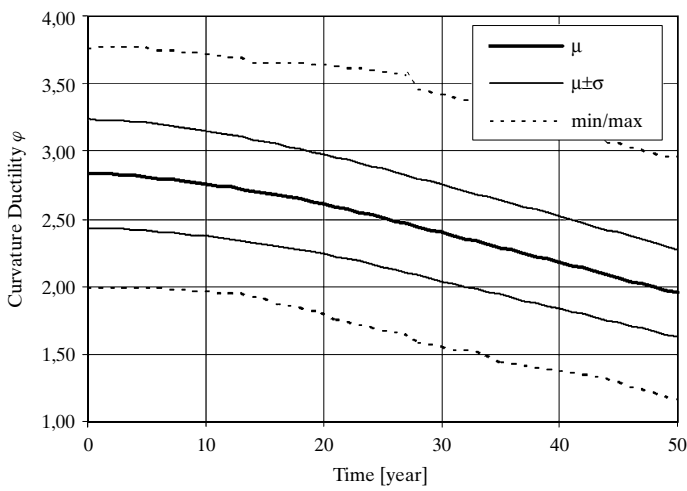


(a) Damaged structure

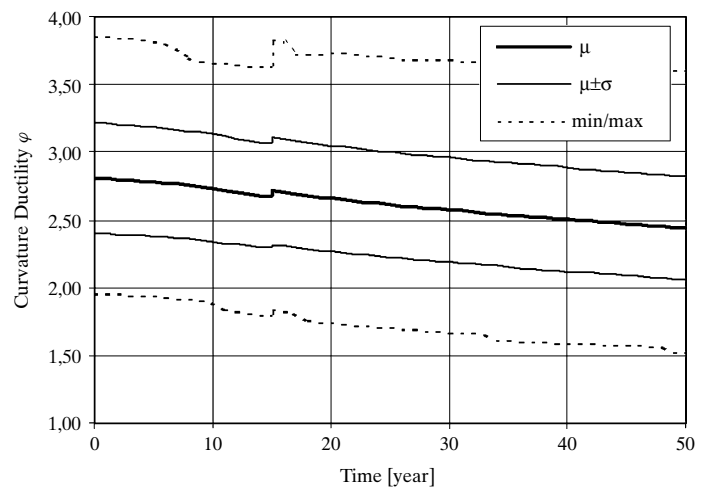


(b) Rehabilitated structure

Fig. 12: Time evolution of the yielding bending moment: mean μ (thick line), standard deviation σ from the mean μ (thin lines), minimum and maximum values (dotted lines)



(a) Damaged structure



(b) Rehabilitated structure

Fig. 13: Time evolution of the curvature ductility: mean μ (thick line), standard deviation σ from the mean μ (thin lines), minimum and maximum values (dotted lines)

Random Variable ($t = t_0$)	Distribution Type	μ	σ
Concrete strength, f_c	Lognormal	$f_{c,nom}$	5 MPa
Steel strength, f_{sy}	Lognormal	$f_{sy,nom}$	30 MPa
Coordinates of the nodal points, (y_i, z_i)	Normal	$(y_i, z_i)_{nom}$	5 mm
Coordinates of the steel bars, (y_m, z_m)	Normal	$(y_m, z_m)_{nom}$	5 mm
Diameter of the steel bars, \varnothing_m	Normal (*)	$\varnothing_{m,nom}$	$0,10\varnothing_{m,nom}$
Diffusion coefficient, D	Normal (*)	D_{nom}	$0,10 D_{nom}$
Concrete damage rate, q_c	Normal (*)	$q_{c,nom}$	$0,30 q_{c,nom}$
Steel damage rate, q_s	Normal (*)	$q_{s,nom}$	$0,30 q_{s,nom}$

(*) Truncated distributions with non negative outcomes are adopted in the simulation process.

Table 1: Probability distributions and their parameters

the two investigated scenarios, Figs. 12 and 13 show the time evolution of the statistical parameters (mean value μ , standard deviation σ , minimum and maximum values) of the performance indicators during the first 50 years of service life. The direct comparison of Figs. 12a and 12b, as well as of Figs. 13a and 13b, demonstrates the high effectiveness of the adopted rehabilitation intervention. In particular, it can be noted that the effects of randomness lead (a) to reduce the magnitude of the instantaneous increase of structural performance, especially in terms of yielding moment, and (b) to better emphasize the delayed beneficial effects of rehabilitation. In fact, beside a relevant increase of performance over time in terms of both yielding moment and curvature ductility, a noteworthy decrease in the dispersion of the yielding moment is achieved.

Based on the probability functions $P = P(t)$ associated to failure and computed from the simulation process, the

service life T associated with given failure probability thresholds P^* can be finally computed:

$$T = \min \left\{ (t - t_0) \mid P \leq P^*, \forall t \geq t_0 \right\} \quad (4)$$

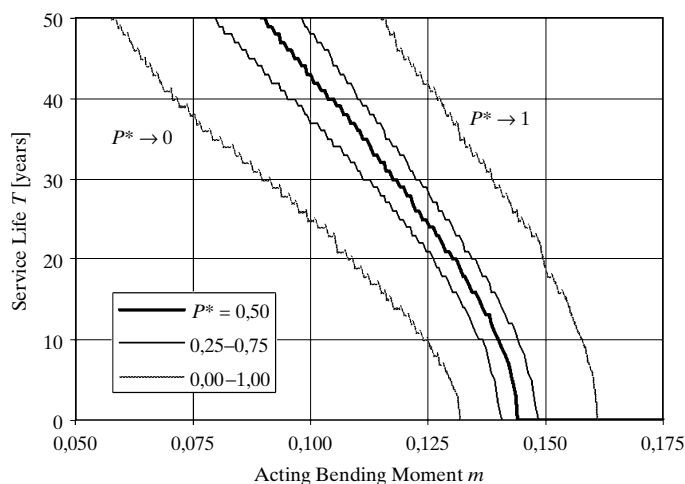
where t_0 is the time instant at the end of the construction phase. Figs. 14 and 15 show the service life T associated with the five reliability levels $P^* = [0,00, 0,25, 0,50, 0,75, 1,00]$ as a function of the expected values of the performance indicators. These curves allow to assess the remaining service life which can be assured under prescribed reliability levels without maintenance. The direct comparison of Figs. 14a and 14b, as well as of Figs. 15a and 15b, shows how the rehabilitation intervention is able to extend the service life of the structure. As an example, for a dimensionless acting bending moment $m \cong 0,10$ and a failure probability threshold $P^* \rightarrow 0$, the service life is extended from $T \cong 25$ years (Fig. 14a) to $T \cong 50$ years (Fig. 14b).

Conclusion

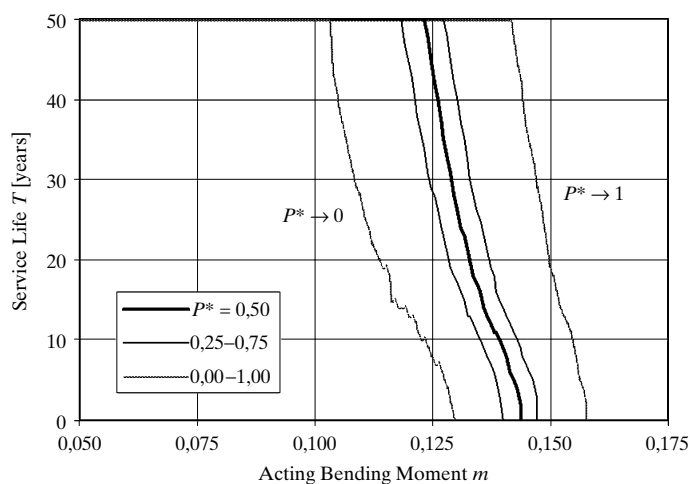
In this study, the time-variant structural performance of an existing cable-stayed bridge under the attack of aggressive agents has been investigated. The effects of a rehabilitation intervention carried out after fifteen years of lifetime have been also taken into account. Differently from the more usual approaches to durability analysis of concrete structures, which generally focus on the local deterioration of the materials only, the proposed methodology allows to evaluate the global effects of the local damaging phenomena on the overall performance of the structure.

In this context, both the deterministic and probabilistic time-variant performances of the Certosa cable-stayed bridge have been analyzed considering two separate cases: without and with rehabilitation intervention. The direct comparison of the results demonstrated that the adopted rehabilitation intervention leads not only to an increase of structural performance over time, but, mainly, to a relevant decrease of the rate of deterioration and, consequently, to a significant reduction of the costs related to future inspections and maintenance actions. In addition, a decrease in the dispersion of the involved uncertainty is also achieved. From the probabilistic point of view this reduction in uncertainty clearly allows a more reliable maintenance planning of the rehabilitated structure.

Finally, the results of the probabilistic investigation have been used to assess the remaining service life which can be assured under prescribed reliability

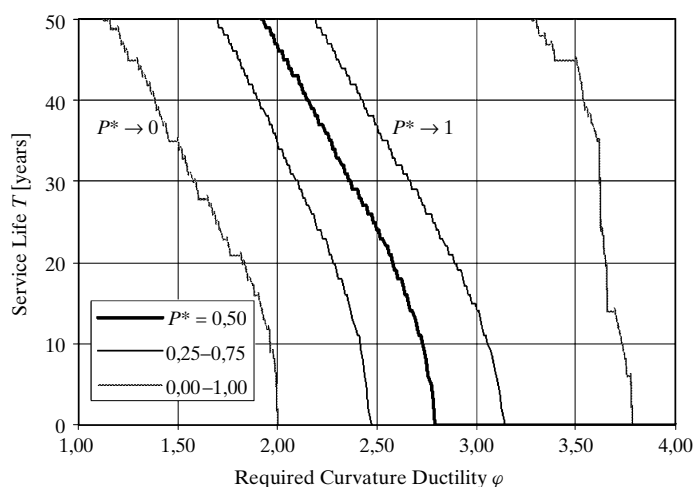


(a) Damaged structure

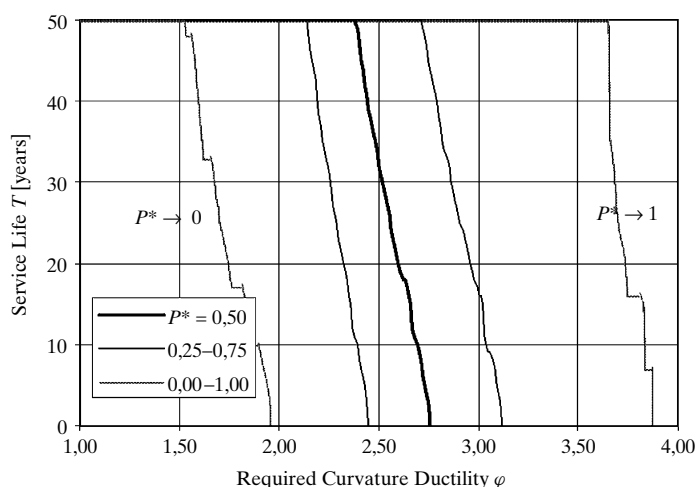


(b) Rehabilitated structure

Fig. 14: Service life associated with prescribed values of probability of failure P^* versus given target levels of the yielding bending moment



(a) Damaged structure



(b) Rehabilitated structure

Fig. 15: Service life associated to given values of probability of failure P^* versus given target levels of the curvature ductility

levels without further maintenance interventions. Even though the accuracy of the results depends on the values of the material parameters which define both the diffusive and damage processes, it is expected that such predictions provide a valuable basis towards a rational planning of future maintenance activities.

Acknowledgements

The Certosa cable-stayed bridge was designed by Francesco Martinez y Cabrera, together with the S.P.E.A. Engineering Technical Office and with the collaboration of Pier Giorgio Malerba for specific structural analysis problems.

References

[1] CEB. *Durable Concrete Structures – Design Guide*, T. Telford, 1992.

[2] BIONDINI, F.; BONTEMPI, F.; FRANGOPOL, D. M.; AND MALERBA, P. G. Cellular Automata Approach to Durability Analysis of Concrete Structures in Aggressive Environments. *ASCE Journal of Structural Engineering*, 130(11), pp. 1724–1737, 2004.

[3] BIONDINI, F.; BONTEMPI, F.; FRANGOPOL, D. M.; AND MALERBA, P. G. Probabilistic Service Life Assessment and Maintenance Planning of Concrete Structures. *ASCE Journal of Structural Engineering*, 132 (5), 2006, pp. 810–825.

[4] BIONDINI, F.; FRANGOPOL, D. M.; AND MALERBA, P. G. Reliability Analysis of a Cable-Stayed Bridge with Damaged Pylons. *9th ASCE Specialty Conference on Probabilistic Mechanics and Structural Reliability*. Albuquerque (NM), USA, July 26–28, 2004.

[5] BIONDINI, F.; FRANGOPOL, D. M.; AND MALERBA, P. G. Lifetime Probabilistic Performance of a Rehabilitated Cable-Stayed Bridge. *4th International Workshop on Life-Cycle Cost Analysis and Design of Civil Infrastructure*

Systems. Cocoa Beach (FL), USA, May 8–11, 2005.

[6] MARTINEZ Y CABRERA, F. *Collected Papers – In memory of Francesco Martinez Y Cabrera*, Politecnico di Milano, 421–426, 2002 (reprinted from *L'Industria Italiana del Cemento*, 643, 1990), 427–436 (reprinted from *Proceedings of Giornate AICAP*, 1993).

[7] MARTINEZ Y CABRERA, F.; MALERBA, P. G.; BONTEMPI, F.; AND BIONDINI, F. Creep Effects on Prestressed Cable Stayed Bridges. *7th International Conference on Computing in Civil and Building Engineering*, 1, Seoul, August 19–21, 1997, pp. 467–472.

[8] GLICKSMAN, M. E. *Diffusion in Solids*, John Wiley and Sons, 2000.

[9] WOLFRAM, S. *Cellular Automata and Complexity – Collected Papers*, Addison-Wesley, 1994.